Table 1
Imuunolabeling pattern of 14-3-3 isoforms in four distinct inclusions

	Pick body (Pick BD)	NFTs (AD) [16]	GCI and NCI (MSA) [9]
14-3-3 proteins	++	++	+
Sigma isoform	+ (D: ++)	+	SI
Zeta	+	++	+
Beta	+	+	+
Gamma	+	+	+
Epsilon	+	+	+
Eta	+	+	NE
Tau	+	+	NE

+: positive; ++: strongly positive; Pick BD: Pick body disease; AD: Alzheimer's disease; MSA: multiple system atrophy; D: inclusions in granule cells in dentate gyrus; GCI: glial cytoplasmic inclusions; NCI: neuronal cytoplasmic inclusions; SI: scarcely immunostained; NE: not examined.

It is interesting if different functions of 14-3-3 proteins are related to difference in their isoforms, because each isoform has different functions under different conditions [6,16,17]. We then used a panel of antibodies specific for each isoform of 14-3-3 proteins. Table 1 shows immunolabeling profile of each isoform of four distinct inclusions. Zeta isoform is preferentially accumulated in NFTs in AD brains while sigma isoform is abundant in Pick bodies in dentate granule cells. This difference suggests that 14-3-3 proteins and its isoforms are differently expressed in different pathological conditions, probably involved in different processes. It was unexpected that Pick bodies are immunopositive for the sigma isoform, because the expression of this isoform has been considered to be limited to extraneuronal cells outside the nervous system [3]. We were, however, successful in demonstrating in normal brain tissue a single band (Fig. 1A) and neuronal labeling (Fig. 2A, E and F) both immunoreactive for sigma isoform and absorbed upon coincubation with the antigen peptide. Preferential accumulation of 14-3-3 protein and its relation to isoform is summarized as Table 1. Possible accumulation of sigma isoform in pathological deposits such as Pick body is in agreement with a previous observation by Kawamoto et al. [9] that glial and neuronal cytoplasmic inclusions in multiple system atrophy are scarcely positive for sigma isoform. Further studies using isoform-specific antibodies is necessary if isoform-specificity has pathological relevance to deposit formation shared by these neurodenerative conditions (Table 1). Growing body of evidence, however, suggests that potential functions of this group of proteins are too variable to be interpreted, at least at present, on unified hypothesis to explain these degenerative processes.

Molecular, as well as topographical, dissection of 14-3-3 proteins and its isoforms in relation to normal and pathological functions and structures will provide us with improved understanding of this molecule.

Acknowledgments

This work is supported in part by grants for Sumitimo Welfare Foundation. We are grateful to Dr. Kazuko Aoki-Yoshino for her help for Western blotting.

References

[1] A. Agarwal-Mawal, H.Y. Qureshi, P.W. Cafferty, Z. Yuan, D. Han, R. Lin, H.K. Paudel, 14-3-3 connects glycogen synthase kinase-3β to tau within a brain microtubule-associated tau phosphorylation complex, J. Biol. Chem. 278 (2003) 12722–12728.
[2] K. Aoki, T. Uchihara, N. Sanjo, A. Nakamura, K. Ikeda, K. Tsuchiya, Y. Wakayama, Increased expression of neuronal apolipoprptein E in human brain with cerebral infarction, Stroke 34 (2003) 875–880.
[3] D. Berg, C. Holzmann, O. Riess, 14-3-3 proteins in the nervous system, Nat. Rev. Neurosci. 4 (2003) 752–762.
[4] I. Ferrer, M. Barrachina, B. Puig, Glycogen synthase kinese-3 is associated with neuronal and glial hyperphosphorylated tau deposits in Alzheimer's disease, Pick's disease, progressive supranuclear palsy and coticobasal degeneration, Acta Neuropathol. 104 (2002) 583–591.
[5] H. Fu, R.R. Subramanian, S.C. Masters, 14-3-3 proteins: structure, function, and regulation, Annu. Rev. Pharmacol. Toxicol. 40 (2000) 617–647.
[6] M. Hashiguchi, K. Sobue, H.P. Paude, 14-3-3 ζ is an effector of tau protein phosphorylation, J. Biol. Chem. 275 (2000) 25247–25254.
[7] G. Hsich, K. Kenney, C.J. Gibbs, K.H. Lee, M.G. Harrington, The 14-3-3 protain in cerebrospinal fluid as a maker for transmissible spongiform encephalopathy, N. Engl. J. Med. 335 (1996) 924–930.
[8] T. Ichihara, T. Isobe, T. Okuyama, T. Yamauchi, H. Fujisawa, Brain 14-3-3 protein is an activator protein that activates tryptophan 5-monooxygenase and tyrosin 3-monooxygenase in the presence of Ca^{2+}, calmodulin-dependent protein kinase II, FEBS Lett. 219 (1987) 79–82.
[9] Y. Kawamoto, I. Akiguchi, S. Nakamura, H. Budka, Accumulation of 14-3-3 proteins in glial cytoplasmic inclusions in multiple system atrophy, Ann. Neueol. 52 (2002) 722–731.
[10] Y. Kawamoto, I. Akiguchi, S. Nakamura, Y. Honjyo, H. Shibasaki, H. Budka, 14-3-3 proteins in Lewy bodies in Parkinson disease and diffuse Lewy body disease brain, J. Neuropathol. Exp. Neurol. 61 (2002) 245–253.
[11] T. Komori, K. Ishizawa, N. Arai, T. Hirose, T. Mizutani, M. Oda, Immunoexpression of 14-3-3 proteins in glial cytoplasmic inclusions of multiple system atrophy, Acta Neuropathol. 103 (2003) 66–70.
[12] R. Layfield, J. Fergusson, A. Aitken, J. Lowe, L. Landon, Neurofibrillary tangles of Alzheimer's disease brain contain 14-3-3 protein, Neurosci. Lett. 209 (1996) 57–60.
[13] M. Rosenquist, 14-3-3 proteins in apoptosis, Braz. J. Med. Biol. Res. 36 (2003) 403–408.
[14] K. Tsuchiya, M. Ikeda, K. Hasegawa, T. Fukui, T. Kuroiwa, C. Haga, S. Oyanagi, I. Nakano, M. Matsushita, S. Yagishita, K. Ikeda, Distribution of cerebral cortical lesions in Pick's disease with Pick bodies: clinicopathological study of six autopsy cases showing unusual clinical presentation, Acta Neuropathol. 102 (2001) 553–571.
[15] T. Uchihara, K. Ikeda, K. Tsuchiya, Pick body disease and Pick syndrome, Neuropathology 23 (2003) 318–326.
[16] T. Umahara, T. Uchihara, K. Tsuchiya, A. Nakamura, T. Iwamoto, K. Ikeda, M. Takasaki, 14-3-3 proteins and zeta isoform containing neurofibrillary tangles in patients with Alzhrimer's disease, Acta Neuropathol. (published online July 2004).
[17] H. Wakabayashi, M. Yano, N. Tachikawa, S. Oka, M. Maeda, H. Kido, Increased concentration of 14-3-3 epsilon, gamma, and zeta isoforms in cerebrospinal fluid of AIDS patients with neuronal destruction, Clin. Chim. Acta 312 (2001) 97–105.
[18] J. Zha, H. Harada, E. Yang, J. Jockel, S.J. Korsmeyer, Serine phosphorylation of death agonist BAD in response to survival factor results in binding to 14-3-3 not BCL-X(L), Cell 87 (1996) 619–692.

RESEARCH ARTICLE

Profound Cardiac Sympathetic Denervation Occurs in Parkinson Disease

Takeshi Amino[1,2,5]; Satoshi Orimo[1,2]; Yoshinori Itoh[3]; Atsushi Takahashi[4]; Toshiki Uchihara[2]; Hidehiro Mizusawa[5]

[1] Department of Neurology, Kanto Central Hospital, Tokyo, Japan.
[2] Department of Neuropathology, Tokyo Metropolitan Institute for Neuroscience, Japan.
[3] Department of Internal Medicine, [4]Department of Organ and Function Pathology, Yokufukai Geriatric Hospital, Tokyo, Japan.
[5] Department of Neurology and Neurological Science, Tokyo Medical and Dental University, Japan.

Corresponding author:
Satoshi Orimo, MD., Department of Neurology, Kanto Central Hospital, 6-25-1 Kami-Yoga, Setagaya-ku, 158-8531, Tokyo, Japan (E-mail: orimo@kanto-ctr-hsp.com)

In the last few years, cardiac sympathetic dysfunction in Parkinson disease (PD) has been postulated on the basis of decreased cardiac uptake of sympathoneural imaging tracers. However, the pathological substrate for the dysfunction remains to be established. We examined the left ventricular anterior wall from postmortem specimens with immunohistochemical staining for tyrosine hydroxylase (TH), neurofilament (NF) and S-100 protein in PD patients and control subjects, and quantified the immunoreactive areas. As TH-immunoreactive axons nearly disappeared and NF-immunoreactive axons drastically decreased in number, the morphological degeneration of the cardiac sympathetic nerves in PD was confirmed. Quantitative analysis showed that sympathetic nerves were preferentially involved. Triple immunofluorolabeling for NF, TH, and myelin basic protein showed clearly the profound involvement of sympathetic axons in PD. The extent of involvement of the cardiac sympathetic nerves seems likely to be equivalent to that in the central nervous system, including the nigrostriatal dopaminergic system. PD affects the cardiac sympathetic nervous system profoundly as well as nigrostriatal dopaminergic system.

Brain Pathol 2005;15:29-34.

INTRODUCTION

Parkinson disease (PD) is not only a disease of the nigrostriatal dopaminergic system but also a disease of the autonomic nervous system. Therefore, symptoms of autonomic dysfunction such as constipation, orthostatic and postprandial hypotension, dyshidrosis and bladder dysfunction occur commonly in PD (32).

Recent awareness of a decrease in cardiac uptake of [^{123}I]*meta*-iodobenzylguanidine (MIBG) on single photon emission computed tomography (SPECT) or of 6-[^{18}F]fluorodopamine (6F-DA) on positron emission tomography (PET) in PD patients is now attracting increasing attention because this decreased uptake is detectable before other autonomic disturbances are evident (6, 24, 39). Moreover, this decrease is of particular clinical importance because it is usually undetectable in patients with multiple system atrophy (MSA), progressive supranuclear palsy (PSP) (39) or corticobasal degeneration (CBD) (23) and could therefore be helpful in isolating PD from among the various parkinsonian syndromes.

The decreased cardiac uptake of these sympathoneural radiotracers may represent dysfunction of the cardiac sympathetic system in PD (6). Indeed, our recent immunohistochemical study demonstrated a marked decrease in tyrosine hydroxylase (TH)-immunoreactive+ axons in the epicardium of the left ventricular anterior wall in PD patients (22, 25). This pathological finding was considered to represent the involvement of the cardiac sympathetic nerves in PD and presumably accounts for the decreased cardiac uptake of the tracers. However, it remains to be clarified whether morphological depletion of the sympathetic nerves and denervation occurs or whether they are merely functionally involved, and whether TH+ axons are selectively affected.

In this case-control study, we observed neurofilament (NF)-immunoreactive axons coupled with TH+ axons, and quantified the frequency of TH+ axons relative to NF+ axons. In addition, we investigated their relation to myelin and Schwann cells. Triple immunofluorolabeling for NF, TH and myelin basic protein (MBP) demonstrated clearly the profound involvement of TH+ axons in PD patients.

MATERIALS AND METHODS

Subjects. Cardiac tissue samples obtained at autopsy from four PD patients and 5 control subjects were used in this study. Clinical diagnosis of PD was based on dopa-responsive parkinsonian symptoms (tremor, muscle rigidity, akinesia and postural instability). The postmortem examination revealed marked neuronal loss and numerous Lewy bodies in the substantia nigra, locus ceruleus and dorsal vagal nucleus. Five control subjects without parkinsonian symptoms and signs, primary heart disease, diabetes mellitus and peripheral neuropathy, were enrolled. The postmortem examinations confirmed the absence of Lewy bodies in the central nervous system. There was no statistical difference in age between the PD patients and control subjects. (Table 1)

Immunohistochemical staining. The heart tissue was fixed in formalin at autopsy within 48 hours after death. Specimens were obtained from the left ventricular anterior wall and embedded in paraffin. The left ventricular wall was considered preferable for this study because PET or SPECT studies in healthy subjects show uniformly high radioactivity there. Four-micrometer thick sections sliced axially were deparaffinized and stained with hematoxylin and eosin (H&E).

We used the following primary antibodies for immunohistochemical staining: anti-NF (SMI-31, mouse monoclonal, 1:10000 SMI, Baltimore, Md) as a marker

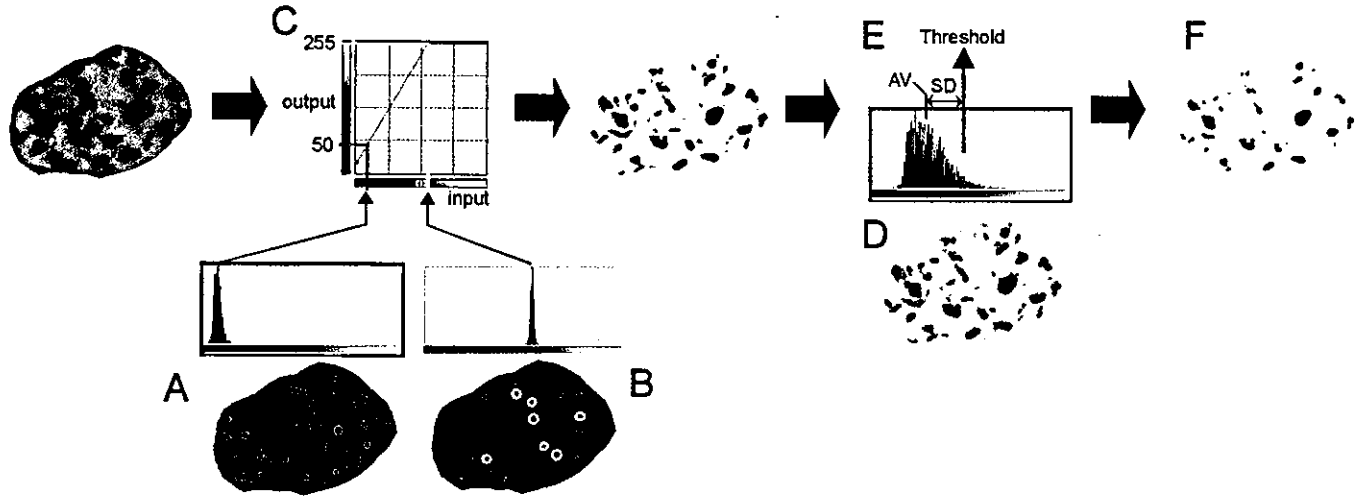

Figure 1. *Procedure for measuring immunoreactive areas.* **A.** On an 8-bit gray scale (0:black-255:white) image, several areas with the most intense immunoreactivity were circled and the mean value of these areas was calibrated to 50 on the 8-bit gray scale. **B.** In the same way, the mean value of several unstained areas was calibrated to 255. **C.** Based on these 2 calibration points, the entire image was transformed linearly into an 8-bit gray scale. **D.** On the transformed image, immunostained axonal areas were arbitrarily selected and their average value (AV) and standard deviation value (SD) were calculated. **E.** The entire image was then binarized with the threshold defined as the AV ± SD. **F.** Areas with a pixel value below the threshold were judged immunoreactive areas. Extracted areas were therefore considered reasonable as immunoreactive areas compared with the original digitalized image.

Case	Age at death	Gender	Duration of disease (years)	Hoehn and Yahr stage	Cause of death
PD 1	70	Male	10	5	Bronchitis
PD 2	82	Female	10	4	Colon cancer, ileus, sepsis
PD 3	83	Female	>3	5	Pneumonia
PD 4	91	Female	15	4	Pneumonia, chronic lymphocytic leukemia
Control 1	86	Female	-	-	Colon cancer
Control 2	89	Male	-	-	Esophageal cancer, pneumonia
Control 3	81	Female	-	-	Colon cancer, peritonitis
Control 4	93	Male	-	-	Acute respiratory failure, tracheitis
Control 5	91	Female	-	-	Acute respiratory failure, emphysema

Table 1. Characteristics of patients and control subjects.

for all axons, anti-TH (mouse monoclonal, 1:3000 SIGMA, Saint Louis, Mo) as a marker for catecholaminergic axons, anti-S-100 protein (mouse monoclonal, 1:1500 IBL, Gunma, Japan) as a marker for Schwann cells and anti-MBP (rabbit polyclonal, 1:1000 IBL) as a marker for myelin. An indirect immunofluorescence procedure using the avidin-biotin technique was employed. The deparaffinized sections were treated in a microwave oven with citrate buffer 3 times for 6 minutes, treated with 1% hydrogen peroxide for 30 minutes and then incubated with the primary antibody diluted with phosphate-buffered saline containing 0.03% Triton-X100 and the corresponding blocking serum. In order to reduce background stain and achieve optimal signal to noise ratio, we usually take 2 days or longer at 4°C for primary antibody incubation with higher dilution. The sections were then incubated for 2 hours with the biotinylated secondary antibody (anti-rabbit or anti-mouse, 1:1000, Vector, Burlingame, Calif), followed by avidin-biotin-peroxidase complex (1:1000 ABC Elite, Vector). The peroxidase labeling was visualized with diaminobenzidine-nickel as chromogen, and then the stained sections were lightly stained with fast nuclear red solution.

Quantification procedure. Relatively large (diameter >50 μm) and round (maximum diameter/minimum diameter <2) nerve fascicles in the epicardium were all selected to quantify the immunoreactive areas. This elimination of oval fascicles (maximum diameter/minimum diameter ≥2) allowed us to avoid quantifying tangentially oriented axons. The selected fascicles were captured by a digital camera (D1, Nikon, Tokyo, Japan) connected to a microscope (BX-50, Olympus, Tokyo, Japan) with an objective ×40. The contour of the endoneurium was traced on a digitizer coupled with a liquid crystal display (PL-400, Wacom, Saitama, Japan). On the digitalized 8-bit RGB image of each endoneurium, the area of the entire endoneurium (fascicle area), TH+ area and NF+ area were measured using a standardized procedure on software (Adobe Photoshop 5.5 and NIH-image 1.62) as shown in Figure 1. Firstly, each digitalized image was transformed into an 8-bit gray scale (0:black-255:white) as follows. Several areas with the most intense immunoreactivity were selected and the mean value of these areas was calibrated to 50 on the 8-bit gray scale. In the same way, the mean value of several unstained areas was calibrated to 255. Based on these 2 calibration points, the entire image was transformed linearly into an 8-bit gray scale. This procedure enabled us to minimize the difference of brightness among the original digitalized images. Based on this transformed image, the average value (AV) and standard deviation value (SD) of stained axonal areas, which were arbitrarily selected, were calculated. The entire image was then binarized with the threshold defined as AV+SD. Areas with a pixel value below the threshold were judged to be immunoreactive areas. Finally the extracted areas were considered reasonable as immunoreactive areas compared with the original digitalized image.

Quantified values from several nerve fascicles from each subject were summed to yield the total fascicle area, total TH+ area and total NF+ area. The ratios of the total TH or NF+ area to the total fascicle area (TH/fascicle of NF/fascicle), the ratio of the total TH+ area to the total NF+ area (TH/NF) and the difference between the total TH+ areas and the total NF+ areas (NF-TH) were calculated for each subject. Differences in these calculated values between the PD and control groups were analyzed with the Mann-Whitney U test.

Triple immunofluorolabeling. Deparaffinized sections from a patient and a control subject were treated in a microwave oven with citrate buffer 3 times for 6 minutes, and then with 2% hydrogen peroxide for 30 minutes. Firstly, they were incubated with the anti-MBP antibody (diluted to 1:9000, which is detectable after catalyzed reporter deposition amplification) at 4°C for 2 days. They were incubated with anti-rabbit IgG made from goat conjugated to horseradish peroxidase (HRP, 1:1000; Pierce, Rockford, Ill). The HRP signal was amplified with biotinylated tyramide (1:1000; Perkin-Elmer, Boston, Mass) and then visualized with Cy-5 conjugated to streptavidin (1:200; Kirkegaard & Perry, Gaithersberg, Md). Subsequently, sections were incubated with a mixture of the anti-NF mouse monoclonal antibody (1:1000) and the anti-TH rabbit polyclonal antibody (1:100) at 4°C for another 2 days in the dark. These 2 antibodies were visualized with a mixture of anti-mouse IgG made from sheep conjugated with rhodamine (1:200, Jackson ImmunoResearch, West Grove, Pa) and anti-rabbit IgG made from goat conjugated with FITC (1:200, Vector), which could selectively visualize the anti-TH antibody because of insufficient sensitivity to the diluted anti-MBP antibody (20, 34).

RESULTS

H&E and immunohistochemical staining (Figure 2). H&E staining of the sections revealed several nerve fascicles, mostly transverse-sectional, in the epicardium. There was no apparent difference in the number and size of those nerve fascicles between the control and PD groups.

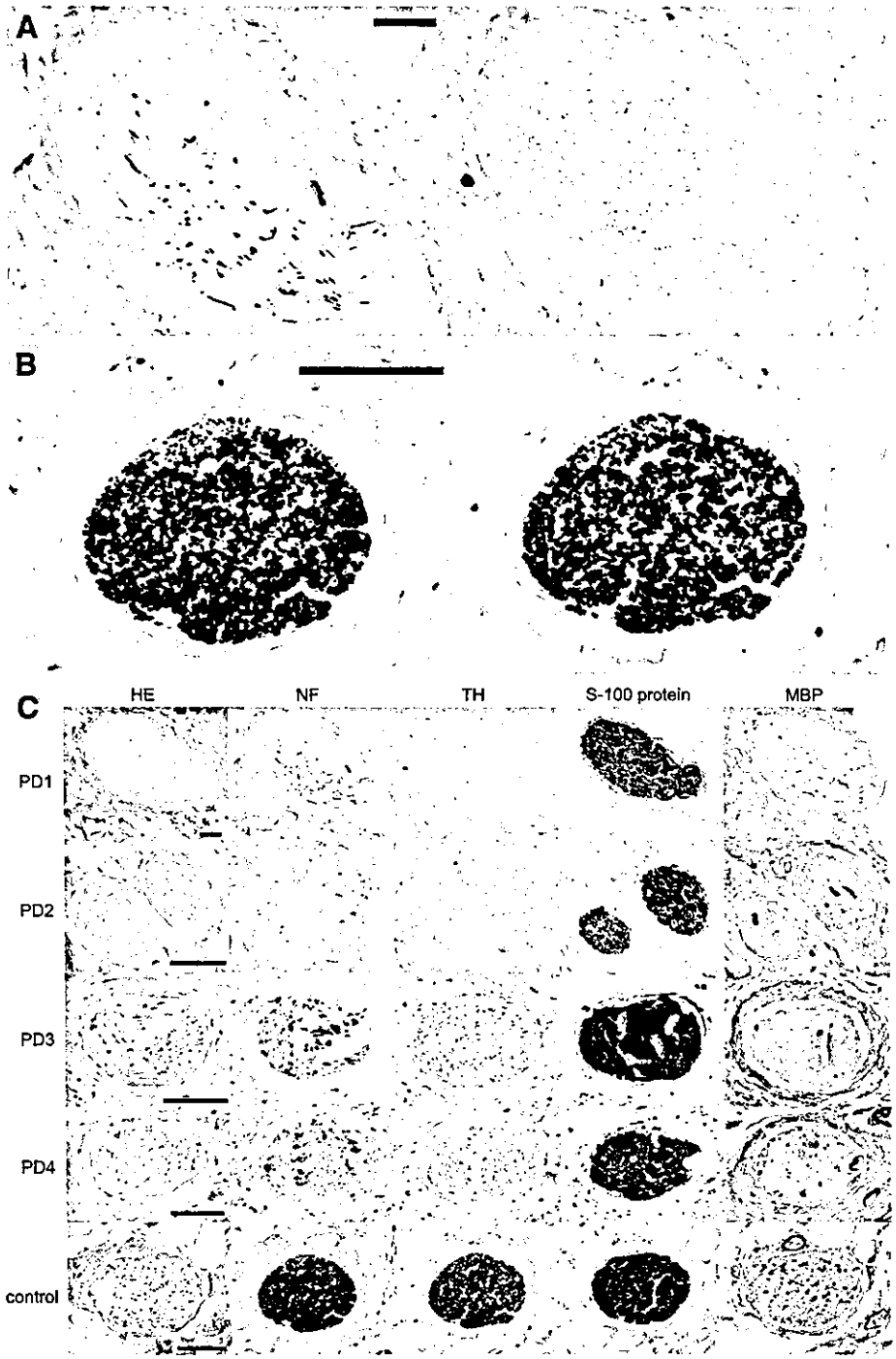

Figure 2. *H&E and immunohistochemical staining.* **A.** In the PD patient (PD 1), neurofilament (NF)-immunoreactive axons (Left) were sparse and tyrosine hydroxylase (TH)-immunoreactive axons (Right) were nearly absent. **B.** The control subject (control 4) showed numerous NF-immunoreactive axons (Left) and TH-immunoreactive axons (Right). **C.** Representative nerve fascicle in each patient or control subject (control 4) were shown. In all patients, NF-immunoreactive axons and TH-immunoreactive axons drastically decreased in number whereas S-100 protein-immunoreactive structures were equally preserved. A few myelin basic protein (MBP)-immunoreactive structures were seen in the fascicles of the epicardium and the number was smaller in patients than in control subjects. Scale bar = 100 μm.

In the control subjects, numerous NF+ axons were shown in the fascicle. Many TH+ axons were also seen, although they were smaller in number than NF+ axons. S-100 protein+ structures were also numerous, whereas MBP+ structures were comparatively sparse.

In the PD patients, NF+ axons were sparse and TH+ axons were nearly absent. A few MBP+ structures were seen, but the

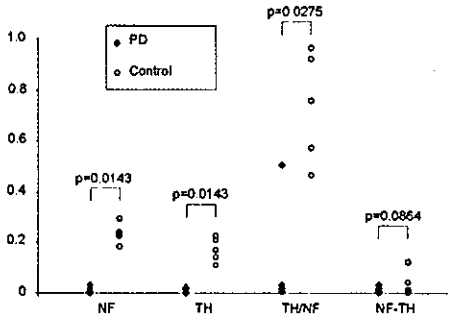

Figure 3. *Results of quantification for immunoreactive areas.* Mann-Whitney U tests were used for the statistical analysis between the patient (PD) and control group(Control).

number was smaller than in the control subjects. S-100 protein+ structures were numerous and equally preserved compared with those in the control subjects.

Quantitative analysis (Figure 3). In the control subjects, the ratios of TH/NF, which were in the range of 47% to 97%, revealed that most of the axons in the nerve fascicles in the epicardium were immunoreactive to TH. Both ratios of TH/fascicle and NF/fascicle obviously and significantly decreased in the PD group. The ratio of TH/NF also significantly decreased in the PD group. On the other hand, the difference of NF-TH showed a tendency to be smaller in the PD group, although it did not reach statistical significance.

Triple immunofluorolabeling (Figure 4). In the control subject (Figure 4B), numerous NF+ axons (red) were observed in nerve fascicles and most were immunoreactive to TH (green). MBP+ structures (blue) were sparse, and some surrounded TH+ axons as well as TH- axons. In the PD patient (Figure 4A), a fairly small number of NF+ axons and fewer MBP+ structures were recognized but TH+ axons were absent.

DISCUSSION

In the last few years, cardiac sympathetic dysfunction in PD has been revealed by the decreased cardiac uptake of sympathoneural tracers detected in SPECT or PET studies. We recently reported a marked decrease in TH+ axons in PD patients based on histological examination of the epicardium of the left ventricular anterior wall. Furthermore, in this case-control study, we expanded this observation by quantifying TH+ axons and NF+ axons in a series of patients with or without PD.

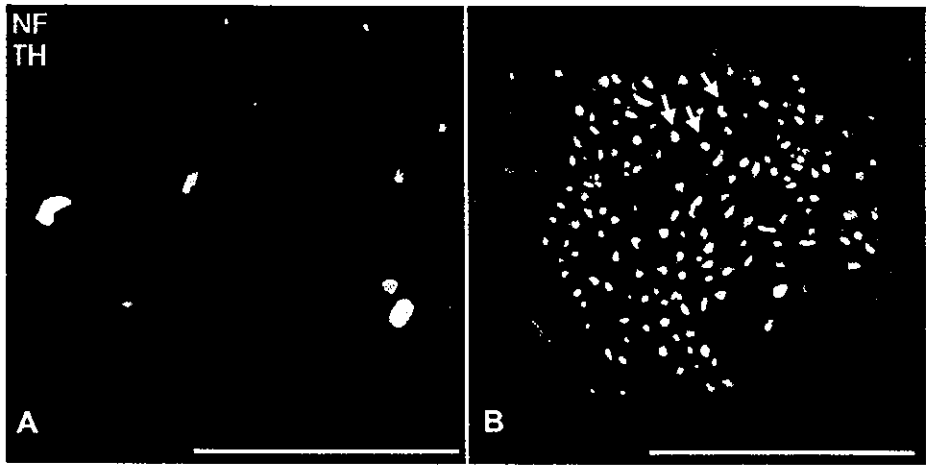

Figure 4. *The nerve fascicles in the epicardial spaces immunofluorolabeled with anti-NF (red), anti-TH (green) and anti-MBP (blue) antibodies.* **A.** PD patient. **B.** Control subject. In PD (**A**), TH-immunoreactive nerve fibers almost disappeared, and NF-immunoreactive nerve fibers and MBP-immunoreactive structure were markedly decreased. In the control subject (**B**), most NF-immunoreactive nerve fibers were also immunoreactive to TH (yellow), and, some were surrounded by MBP-immunoreactive structures (arrow in B). Scale bar = 50 μm.

Immunohistochemical staining revealed that the nerve fascicle in the epicardium contains a large number of TH+ axons in normal individuals. The high proportion of TH/NF in quantitative analysis indicated that TH+ axons occupy more than half of all axons in each fascicle. This TH+ dominant proportion is consistent with the previously reported ratio of catecholaminergic axons to cholinergic axons in the ventricular myocardium (2, 11). TH is a rate-limiting enzyme in catecholamine synthesis. The presence of TH in an axon is considered to indicate that the axon is catecholaminergic, and it has been used as a marker for locating presumptive sympathetic neural tissue (18). Recent studies demonstrated that TH could be also present in non-sympathetic tissue, such as the cranial parasympathetic ganglia of rat (9) or human cardiac ganglia (31), while its functional relevance in relation to the nature of the axons remains speculative. The existence of TH, therefore, is unable to prove conclusively by itself that the tissue is sympathetic. However, in the myocardium, noradrenalin is the dominant species among catecholamines (21, 28) and its tissue concentration is drastically reduced after stellectomy in rats (14, 27) and guinea pigs (7). This suggests that TH+ axons in the epicardium of the left ventricle presumably represent sympathetic axons, mainly noradrenergic axons originating from the cervico/thoracic sympathetic ganglia. The disappearance of TH+ axons in transplanted human hearts (30, 37) also indicates that TH+ axons are extrinsic, and is compatible with this interpretation.

The immunohistochemical staining for NF and TH showed a drastic decrease of NF+ axons and a more profound decrease of TH+ axons in PD. This finding indicated not merely the loss of the catecholamine synthesis enzyme, TH, but also the depletion of the sympathetic axons themselves. It means that the cardiac sympathetic nerves are morphologically degenerated. This offered new morphological evidence for the involvement of the cardiac sympathetic nerves in addition to the functional evidence that had been shown by PET or SPECT studies.

The near complete disappearance of TH+ axons and significant decrease in TH/NF in the PD group show that the sympathetic nerves were profoundly and preferentially involved in PD patients. On the other hand, NF-TH, that represents TH- axons, tended to be less frequent in PD, although the difference was not statistically significant. It is therefore possible that TH- axons are not involved. The PD related-depletion of TH- axons, if present, could have been overlooked because of the small number of TH- axons, leaving the possibility that the non-catecholaminergic axon is also involved in PD. Although the origin and nature of these non-catecholaminergic axons remain speculative, they may be from intrinsic neurons where Lewy bodies were previously found (10, 36).

According to PET or SPECT study, the extent of involvement in PD seems to vary

in the sympathetic nervous system. Decreased uptake of the tracers, 6F-DA or MIBG, was noted only in the heart, the thyroid gland and renal cortex, and the decrease in the heart was most prominent (5, 6, 29, 33). Moreover, there also seem to be differences among the parts of the heart. The PET study revealed that 6F-DA radioactivity was more severely decreased in the left ventricular free-wall than in the interventricular septum or the right myocardium (6, 12). Thus, the left ventricular anterior wall was expected to be one of the parts where the sympathetic nerve was most severely affected. We investigated this part of the heart pathologically and ascertained that the sympathetic nerves nearly disappeared.

There are several reports quantifying the TH protein content or TH activity in the central nervous system on postmortem examinations in PD. The TH protein content in PD decreased to 2.7% in the caudate nucleus, 5.3% in the putamen and 16% in substantia nigra compared with the control (17). TH activity decreased to 9.2% to 27.4% in the caudate nucleus, 4.1% to 21.6% in the putamen, 11.9% to 35.1% in the substantia nigra, 11.6% to 50.7% in the globus pallidus and 13% in the locus ceruleus (13, 16, 19). Our study revealed that in the epicardium of the left ventricular anterior wall, TH+ axons nearly completely disappeared in PD and the TH/fascicle ratio measured by quantitative analysis decreased to 1.1% of the control. Although there are differences in the measured object, it can be said that the cardiac sympathetic nerves in the left ventricular anterior wall are affected as much as the dopaminergic nerves in the central nervous system.

The sympathetic innervation to the ventricular working myocardium is thought to be mainly through the para-arterial route in the epicardium (15), consistent with the observation that the number of TH+ axons in the subepicardial area were larger than in the subendocardial area (11). The nerve fascicles in the epicardium, therefore, presumably contain sympathetic efferent axons innervating the working myocardium from the cervico/thoracic sympathetic ganglia. The depletion of TH+ axons in the epicardium represents the effacement of their distal axons and terminals, and therefore indicates cardiac sympathetic denervation in PD. The decreased cardiac uptake of these tracers is assumed to result from the effacement of these terminals since 6F-DA and MIBG are taken up by and stored in the adrenergic nerve terminals as with catecholamines (1, 38).

In addition, our study showed small number of myelinated axons in the epicardium, and the triple immunofluorolabeling unexpectedly demonstrated that some of the TH+ axons, although very small in number, were myelinated. The postganglionic sympathetic axons are generally considered unmyelinated C-fiber (35). Although the sympathetic afferent nerves consist of unmyelinated axons, it is uncertain and doubtful whether they are catecholaminergic. Neurotransmitters in the sympathetic afferent nerves are presumably considered substance P or neuropeptide K (26). As there was a report suggesting the existence of myelinated sympathetic postganglionic axons in a cat (3), our observation may indicate that the cardiac postganglionic sympathetic nerve contains tiny numbers of myelinated axons in humans.

In considering the pathogenesis of PD, the cardiac sympathetic nerves have not been emphasized as much as the central nervous system. This may be due to clinical absence of cardiac manifestations and the difficulty in detecting abnormalities. Because physiological functions of these sympathetic fibers in the myocardium are not well characterized, it is hard to predict the outcome after their depletion. Although diminished heart rate variability spectral measures of the variability have been reported in PD (8), routine electrocardiogram or ultrasound cardiography usually fail to demonstrate abnormalities. Indeed, all thirty-six PD patients in our previous study with decreased cardiac uptake of MIBG showed normal left ventricular function by ultrasound cardiography and most of them did not show serious arrhythmias and ST changes by 24-hour Holter electrocardiography (24). Among four PD patients in the present study, asymptomatic second degree A-V block of Mobitz type was the only abnormality in cardiac function. Because decreased cardiac uptake is not necessarily correlated with the presence of orthostatic hypotension nor with cardiac dysfunctions (5, 24), it is possible that near complete absence of sympathetic axons, first identified in the present study, is not related to clinically detectable manifestations. This is in agreement with the observation that left ventricular functions of transplanted heart under resting condition are quite normal even before sympathetic innervation is re-established (4). However, we should pay attention that decreased motor activity in PD patients may allow cardiac abnormalities, even if present, to remain unnoticed. Awareness of this sympathetic denervation, however, may raise attention to cardiac functions in PD patients and give clues to identify more subtle changes of cardiac functions so far not detectable but possibly linked to this sympathetic denervation.

This study demonstrated pathologically profound involvement in the cardiac sympathetic nervous system, which is catecholaminergic in common with the nigrostriatal nervous system. This may afford a new clue to elucidating the pathogenesis of PD.

REFERENCES

1. Chiueh CC, Zukowska-Grojec Z, Kirk KL, Kopin IJ (1983) 6-Fluorocatecholamines as false adrenergic neurotransmitters. *J Pharmacol Exp Ther* 225:529-533.

2. Chow LT, Chow WH, Lee JC, Chow SS, Anderson RH, Gosling JA (1998) Postmortem changes in the immunohistochemical demonstration of nerves in human ventricular myocardium. *J Anat* 192:73-80.

3. Emery DG, Foreman RD, Coggeshall RE (1978) Categories of axons in the inferior cardiac nerve of the cat. *J Comp Neurol* 177:301-310.

4. Frank MB, Peter U, Nina S, Stephan GN, Bruno R, Markus S (2001) Myocardial Efficacy and Sympathetic Reinnervation After Orthotopic Heart Transplantation. *Circulation* 103:1881-1886

5. Goldstein DS, Holmes CS, Dendi R, Bruce SR, Li ST (2002) Orthostatic hypotension from sympathetic denervation in Parkinson's disease. *Neurology* 58:1247-1255.

6. Goldstein DS, Holmes C, Li ST, Bruse S, Metman LV, Cannon RO (2000) Cardiac sympathetic denervation in Parkinson disease. *Ann Intern Med* 133:338-347.

7. Goto K, Longhurst PA, Cassis LA, Head RJ, Taylor DA, Rice PJ, Fleming WW (1985) Surgical sympathectomy of the heart in rodents and its effect on sensitivity to agonists. *J Pharmacol Exp Ther* 234:280-287.

8. Haapaniemi TH, Pursiainen V, Korpelainen JT, Huikuri HV, Sotaniemi KA, Myllyl VV (2001) Ambulatory ECG and analysis of heart rate variability in Parkinson's disease. *J Neurol Neurosurg Psychiatry* 70:305-310

9. Hardebo JE, Suzuki N, Ekblad E, Owman C (1992) Vasoactive intestinal polypeptide and acetylcholine coexist with neuropeptide Y, dopamine-beta-hydroxylase, tyrosine hydroxylase, substance P or calcitonin gene-related peptide in

neuronal subpopulations in cranial parasympathetic ganglia of rat. *Cell Tissue Res* 267:291-300.

10. Iwanaga K, Wakabayashi K, Yoshimoto M, Tomita I, Satoh H, Takashima H, Satoh A, Seto M, Tsujihata M, Takahashi H (1999) Lewy body-type degeneration in cardiac plexus in Parkinson's and incidental Lewy body diseases. *Neurology* 52:1269-1271.

11. Kawano H, Okada R, Yano K (2003) Histological study on the distribution of autonomic nerves in the human heart. *Heart Vessels* 18:32-39.

12. Li ST, Dendi R, Holmes C, Goldstein DS (2002) Progressive loss of cardiac sympathetic innervation in Parkinson's disease. *Ann Neurol* 52:220-223.

13. Lloyd KG, Davidson L, Hornykiewicz O (1975) The neurochemistry of Parkinson's disease: effect of L-dopa therapy. *J Pharmacol Exp Ther* 195:453-464.

14. Maccarrone C, Jarrott B (1987) Differential effects of surgical sympathectomy on rat heart concentrations of neuropeptide Y-immunoreactivity and noradrenaline. *J Auton Nerv Syst* 21:101-107.

15. Martins JB, Zipes DP (1980) Epicardial phenol interrupts refractory period responses to sympathetic but not vagal stimulation in canine left ventricular epicardium and endocardium. *Circ Res* 47:33-40.

16. McGeer PL, McGeer EG (1976) Enzymes associated with the metabolism of catecholamines, acetylcholine and gaba in human controls and patients with Parkinson's disease and Huntington's chorea. *J Neurochem* 26:65-76.

17. Mogi M, Harada M, Kiuchi K, Kojima K, Kondo T, Narabayashi H, Rausch D, Riederer P, Jellinger K, Nagatsu T (1988) Homospecific activity (activity per enzyme protein) of tyrosine hydroxylase increases in parkinsonian brain. *J Neural Transm* 72:77-82.

18. Molinoff PB, Axelrod J (1971) Biochemistry of catecholamines. *Annu Rev Biochem* 40:465-500.

19. Nagatsu T, Yamaguchi T, Rahman MK, Trocewicz J, Oka K, Hirata Y, Nagatsu I, Narabayashi H, Kondo T, Iizuka R (1984) Catecholamine-related enzymes and the biopterin cofactor in Parkinson's disease and related extrapyramidal diseases. *Adv Neurol* 40:467-473.

20. Nakamura A, Uchihara T (2004) Dual enhancement of triple immunofluorescence using two antibodies from the same species. *J Neurosci Methods* 135:67-70.

21. Neubauer B, Christensen NJ (1976) Norepinephrine, epinephrine, and dopamine contents of the cardiovascular system in long-term diabetics. *Diabetes* 25:6-10.

22. Orimo S, Oka T, Miura H, Tsuchiya K, Mori F, Wakabayashi K, Nagao T, Yokochi M (2002) Sympathetic cardiac denervation in Parkinson's disease and pure autonomic failure but not in multiple system atrophy. *J Neurol Neurosurg Psychiatry* 73:776-777.

23. Orimo S, Ozawa E, Nakade S, Hattori H, Tsuchiya K, Taki K, Takahashi A (2003) [^{123}I] metaiodobenzylguanidine myocardial scintigraphy differentiates corticobasal degeneration from Parkinson's disease. *Intern Med* 42:127-128.

24. Orimo S, Ozawa E, Nakade S, Sugimoto T, Mizusawa H (1999) ^{123}I-metaiodobenzylguanidine myocardial scintigraphy in Parkinson's disease. *J Neurol Neurosurg Psychiatry* 67:189-194.

25. Orimo S, Ozawa E, Oka T,Nakade S, Tsuchiya K, Yoshimoto M, Wakabayashi K, Takahashi H (2001) Different histopathology accounting for a decrease in myocardial MIBG uptake in PD and MSA. *Neurology* 57:1140-1141.

26. Owman C (1988) Autonomic innervation of the cardiovascular system. In: *Handbook of Chemical Neuroanatomy*, Bjorklund A, Hokfelt T (eds.), Volume 6, The Peripheral Nervous System, Chapter IX, pp.327-340, Elsevier: Amsterdam, New York, Oxford

27. Pardini BJ, Lund DD, Schmid PG (1990) Innervation patterns of the middle cervical--stellate ganglion complex in the rat. *Neurosci Lett* 117:300-306.

28. Petch MC, Nayler WG (1979) Concentration of catecholamines in human cardiac muscle. *Br Heart J* 41:340-344

29. Reinhardt MJ, Jungling FD, Krause TM, Braune S (2000) Scintigraphic differentiation between two forms of primary dysautonomia early after onset of autonomic dysfunction: value of cardiac and pulmonary iodine-123 MIBG uptake. *Eur J Nucl Med* 27:595-600.

30. Schuurman HJ, Plomp S, Wijngaard PL, Slootweg PJ, de Jonge N (1993) Innervation of the endomyocardium in the first period after heart transplantation. *Transplantation* 56:85-88.

31. Singh S, Johnson PI, Javed A, Gray TS, Lonchyna VA, Wurster RD (1999) Monoamine- and histamine-synthesizing enzymes and neurotransmitters within neurons of adult human cardiac ganglia. *Circulation* 99:411-419.

32. Takahashi A (1991) Autonomic nervous system disorders in Parkinson's disease. *Eur Neurol* 31(Suppl 1):41-47.

33. Taki J, Nakajima K, Hwang EH, Matsunari I, Komai K, Yoshita M, Sakajiri K, Tonami N (2000) Peripheral sympathetic dysfunction in patients with Parkinson's disease without autonomic failure is heart selective and disease specific. *Eur J Nucl Med* 27:566-573.

34. Uchihara T, Nakamura A, Nakayama H, Arima K, Ishizuka N, Mori H, Mizushima S (2003) Triple immunofluorolabeling with two rabbit polyclonal antibodies and a mouse monoclonal antibody allowing three-dimensional analysis of cotton wool plaques in Alzheimer disease. *J Histochem Cytochem* 51:1201-1206.

35. Van Stee EW (1978) Autonomic innervation of the heart. *Environ Health Perspect* 26:151-158.

36. Wakabayashi K, Takahashi H (1997) Neuropathology of autonomic nervous system in Parkinson's disease. *Eur Neurol* 38 Suppl 2:2-7.

37. Wharton J, Polak JM, Gordon L, Banner NR, Springall DR, Rose M, Khagani A, Wallwork J, Yacoub MH (1990) Immunohistochemical demonstration of human cardiac innervation before and after transplantation. *Circ Res* 66:900-912.

38. Wieland DM, Brown LE, Tobes MC, Rogers WL, Marsh DD, Mangner TJ, Swanson DP, Beierwaltes WH (1981) Imaging the primate adrenal medulla with [^{123}I] and [^{131}I] meta-iodobenzylguanidine: concise communication. *J Nucl Med* 22:358-364.

39. Yoshita M (1998) Differentiation of idiopathic Parkinson's disease from striatonigral degeneration and progressive supranuclear palsy using iodine-123-meta iodobenzylguanidine myocardial scintigraphy. *J Neurol Sci* 155:60-67.

Acta Neuropathol (2005) 109: 159–164
DOI 10.1007/s00401-004-0922-3

REGULAR PAPER

Toshiki Uchihara · Charles Duyckaerts
Danielle Seilhean · Ayako Nakamura
Françoise Lazarini · Jean-Jacques Hauw

Exclusive induction of tau2 epitope in microglia/macrophages in inflammatory lesions—tautwopathy distinct from degenerative tauopathies

Received: 13 May 2004 / Revised: 2 August 2004 / Accepted: 2 August 2004 / Published online: 12 November 2004

Abstract Tau2 antibody recognizes a phosphorylation-independent epitope that is pathologically modified as tau protein is phosphorylated to form neurofibrillary tangles of Alzheimer's disease (AD). Similar modification of tau2 epitope can be induced even in the absence phosphorylation of tau, as we first demonstrated in ischemic foci and in glial cytoplasmic inclusions (GCIs) of multiple system atrophy. This modification of tau2 epitope is distinguishable from those observed in degenerative tauopathies because (1) it is a conformational change, which is reversible upon exposure to a detergent; (2) it shows an absence of fibrils composed of phosphorylated tau protein; and (3) it is characterized by the lack of immunohistochemical labeling by anti-tau antibodies other than tau2. In this study, we expanded this observation to inflammatory foci of different pathologies (human immunodeficiency virus encephalopathy, progressive multifocal leukoencephalopathy or multiple sclerosis) by examining formalin-fixed, paraffin-embedded sections immunostained with a panel of anti-tau antibodies. It was found that tau2 was the only anti-tau antibody that immunolabeled microglia/macrophages in these lesions, and this immunoreactivity was reversibly diminished upon exposure to a detergent. Exclusive apparition of tau2 immunoreactivity in these cells without neurofibrillary pathology may be a secondary event shared with ischemic foci and GCIs. It is, however, related to a unique conformational state of tau, possibly grouped under the name of "tautwopathy", that may represent an initial stage of tau deposition distinct from degenerative tauopathies characterized by fibrils composed of phosphorylated tau protein.

Keywords Tauopathy · Tautwopathy · Multiple sclerosis · Progressive multifocal leukoencephalopathy · HIV encephalopathy

T. Uchihara (✉) · A. Nakamura
Department of Neuropathology,
Tokyo Metropolitan Institute for Neuroscience,
2-6 Musashi-dai, Fuchu, 183-8526 Tokyo, Japan
E-mail: uchihara@tmin.ac.jp
Tel.: +81-42-3253881
Fax: +81-42-3218678

T. Uchihara · C. Duyckaerts · D. Seilhean · F. Lazarini
J.-J. Hauw
Laboratoire Raymond Escourolle, Service de Neuropathologie,
Hôpital de la Salpêtrière, Association Claude Bernard,
Université Paris VI, 47 Boulevard de l'Hôpital,
75651 Paris Cedex 13, France

Introduction

Tau deposition is one of the major neuropathological hallmarks for a variety of neurodegenerative disorders, grouped under the name of tauopathy. In our previous immunohistochemical studies on human brains with cerebral infarction, obtained at autopsy, we reported the presence of Alz-50 [22] and tau2 immunoreactivity (IR) [24] in neurons and microglia/macrophages, respectively, and demonstrated that tau deposition was not a specific phenomenon restricted to degenerative tauopathies. Subsequent studies on human brains demonstrated that tau protein in ischemic foci was not phosphorylated, and the tau2 IR was reversibly abolished upon exposure to a detergent [28]. Interestingly, similar changes were observed for glial cytoplasmic inclusions (GCIs) of multiple system atrophy (MSA) [21]. The absence of neurofibrillary changes in these tau2-immunopositive cells in ischemic foci and GCIs indicates that tau deposition, by itself, does not necessarily lead to neurofibrillary changes in human brains. Because modification of tau protein is a prerequisite for immunohistochemical visualization on formalin-fixed, paraffin-embedded sections [12, 18], identification of specific changes in these non-fibrillary tau deposits will potentially clarify differences among a variety of tau deposits. In the present

study, we expanded this observation by examining tau-immunostained sections in the vicinity of inflammatory foci of different pathologies. This is the first study demonstrating that induction of tau2 IR in activated microglia/macrophages, which is distinct from neurofibrillary changes, is a phenomenon shared by a variety of inflammatory processes as well as by ischemia and GCIs of MSA.

Materials and methods

Five cases with human immunodeficiency virus (HIV) encephalopathy (age at death: 23–42 years), four cases with progressive multifocal leukoencephalopathy (PML) (age at death: 35–85 years) and six cases with multiple sclerosis (MS) (age at death: 30–57 years) were enrolled in this study. Formalin-fixed, paraffin-embedded blocks containing active foci with glial reactions were obtained. Deparaffinized sections were treated with 1% H_2O_2 for 20 min followed by blocking with 5% normal serum. The sections were immunostained with one of the anti-tau antibodies (tau2 [16, 17], 1:1,000, Sigma, Saint Louis, MO; AT8 [13], 1:10,000, Innogenetics, Zwinjndrecht, Belgium; anti-human tau (pool 2) [5], 1:10,000, a generous gift from Prof. H. Mori, Osaka City University; tau-1 [17], 1:10,000, Boehringer, Manheim, Germany; or Alz-50, 1:200, a generous gift from Prof. P. Davies [30]) using the avidin-biotin-peroxidase complex (ABC) method with diaminobenzidine and nickel ammonium sulfate as chromogen, which yielded a deep purple reaction product. Specificity of tau2 IR was established previously both on immunoblot and histological sections from human brains [21, 28]. Preabsorption of tau2 antibody with a synthetic peptide corresponding to the tau2 epitope (AGIGDTSNLEDQAA [29] 1 μg/ml) or with the same concentration (1 μg/ml) of Fc fragment of human IgG (Athens Research & Technol Inc, Athens, GA) was performed in parallel. Omission of the primary antibody served as negative control to see whether secondary antibodies (biotinylated anti-mouse IgG or biotinylated anti-human IgG, Vector) yielded nonspecific labeling mediated, for example, through Fc receptors possibly present on microglial cells. The influence of detergent on tau2 IR was examined, as reported previously on human brains with infarction, AD [28], Down's syndrome and MSA [21], by incubating the sections with tau2 antibody diluted in phosphate-buffered saline (PBS) with or without 0.03% polyoxylethyleneglycol-*p*-isooctylphenyl ether (Triton X-100, TX). In parallel, preincubation with PBS containing 0.03% TX was followed by washing with PBS not containing TX before tau2 immunostaining.

When necessary, the tau2-immunostained sections were subsequently subjected to the second cycle immunostaining with either anti-ferritin (rabbit polyclonal, 1:1,000, DAKO, Glostrup, Denmark) or anti-glial fibrillary acidic protein (GFAP; rabbit polyclonal, 1:10,000, DAKO) antibody. Omission of nickel ammonium sulfate from the chromogen yielded a brown reaction product for these second-cycle antibodies. Double immunostaining with two different monoclonal antibodies (anti-gp24 against HIV, DAKO and tau2) was performed as follows [9, 15, 27]. Tau2 antibody was diluted 1:10,000, and was probed by an anti-mouse IgG conjugated with horseradish peroxidase (HRP; 1:1,000, Kirkegaard Perry, Gaithersburg, MD). The HRP signal was amplified using biotinylated tyramide (1:1,000) in the presence of 0.01% H_2O_2 [1]. After incubation with streptavidin-conjugated HRP (1:200, Vector, Burlingame, CA), color development was performed with diaminobenzidine and nickel ammonium sulfate to yield a deep purple reaction product. These tau2-immunostained sections were then subjected to the second-cycle immunostaining with another mouse monoclonal antibody against gp24 using the ABC method. The amplification performed with biotinylated tyramide in the first cycle was so sensitive that the primary antibody tau2 could be diluted to 1:10,000; however, the ABC method used in the second cycle was not sensitive enough to detect this dilution (1:10,000) of tau2 antibody, and exclusively visualized the gp24 epitope. Omission of nickel ammonium sulfate from the chromogen yielded a brown reaction product for the gp24 epitope.

Results

Microglia/macrophages, major components in these inflammatory processes of these brains, contained tau2 IR in all the sections examined, regardless of the diagnosis (Fig. 1A PML, D MS, G HIV encephalopathy). Tau2 IR in these cells was abolished when the primary antibody was diluted in PBS containing 0.03%TX (Fig. 1B, E, H). Disappearance of tau2 IR upon exposure to TX was reversed when the sections, preincubated with 0.03%TX, were washed with PBS not containing TX before immunostaining (Fig. 1C, F, J). This tau2 IR (Fig. 2A, at the periphery of a demyelinating focus of MS) was abolished when the antibody was co-incubated with the synthetic peptide corresponding to its target epitope [29] (Fig. 2B, the same area as Fig. 2A). Co-incubation of the Fc fragment of human IgG with tau2 failed to eliminate this tau2 IR (data not shown). Preincubation of the section with an excess amount (10 μg/ml) of the Fc fragment also failed to eliminate tau2 IR (data not shown). Finally, direct probing of the section either with biotinylated anti-mouse IgG or biotinylated anti-human IgG, followed by ABC method, visualized no IR (data not shown). These data indicate that immunoreaction with tau2 is specific for the tau2 epitope and is not due to nonspecific reactions, for example, mediated by the Fc receptor potentially expressed on the surface of microglial cells. These tau2-immunoreactive cells were not co-labeled with anti-GFAP (Fig. 2C, a lesion of PML), and double labeling

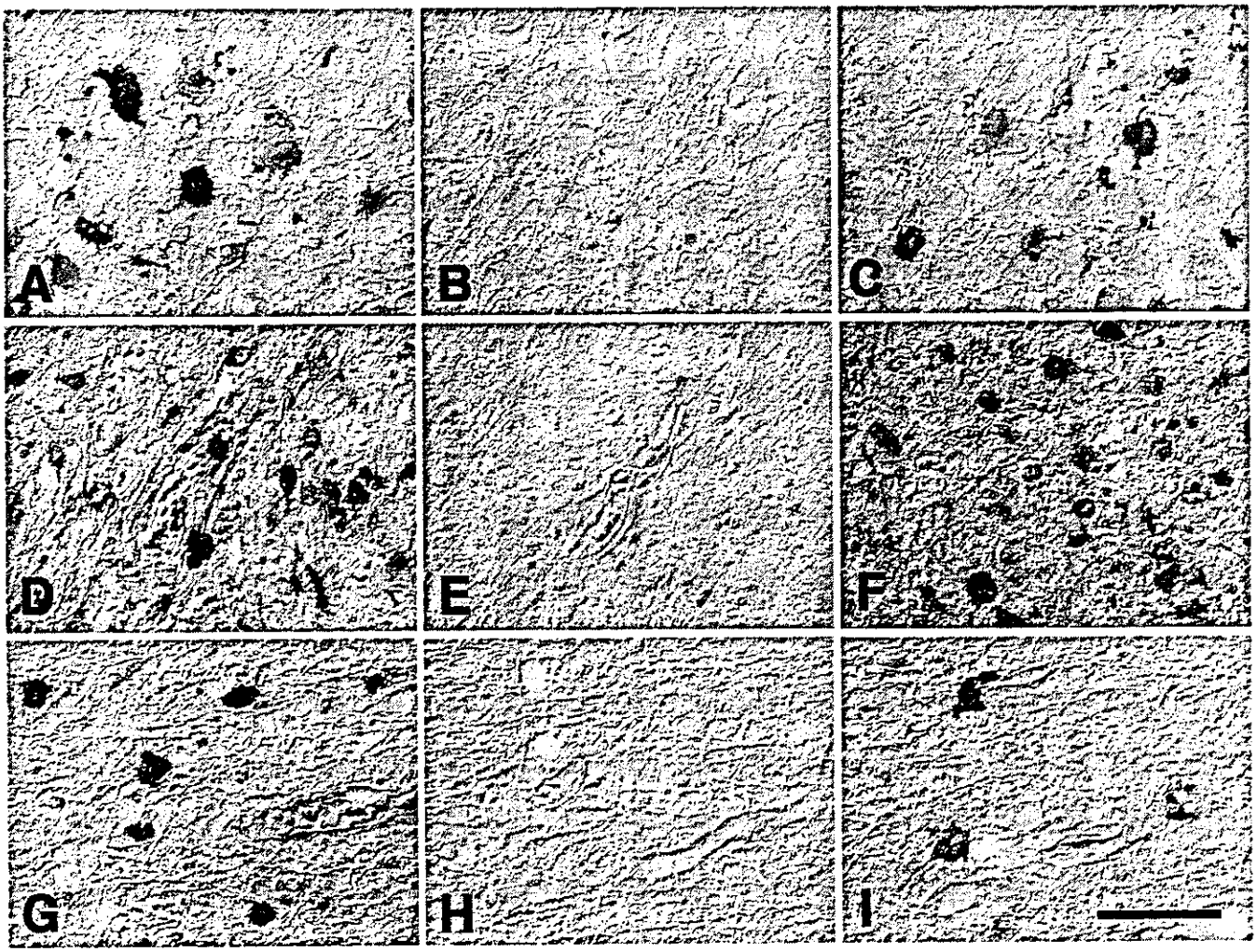

Fig. 1 Tau2-immunoreactive cells in PML (A–C), MS (D–F) and HIV encephalopathy (G–I). Tau2 IR (A PML, D MS, G HIV) is abolished when the primary antibody is diluted in buffer containing 0.03% TX (B PML, E MS, H HIV). This abolished tau2 IR upon exposure to TX (B, E, H) is restored after washing (C, F, I) [*PML* progressive multifocal leukoencephalopathy, *MS* multiple sclerosis, *HIV* human immunodeficiency virus, *IR* immunoreactivity, *TX* Triton X-100 (polyoxylethyleneglycol-*p*-isooctylphenyl ether)]. *Bar* 50 μm

immunohistochemistry with tau2 and anti-ferritin antibody demonstrated the colocalization of these two epitopes (Fig. 2D, HIV encephalopathy), confirming the microglial origin of these tau2-immunopositive cells. In brains with HIV encephalopathy, perivascular aggregates of microglia/macrophages (Fig. 2D) and giant multinucleated cells (Fig. 2E, arrow) contained tau2 IR. Double labeling with tau2 (deep purple) and anti-gp24 (brown) demonstrated that these epitopes were colocalized to microglia/macrophages (Fig. 2E). Modified oligodendrocytes found in PML brains did not exhibit tau2 IR (Fig. 2F, arrow). The panel of anti-tau antibodies other than tau2 failed to immunostain these microglia/macrophages. Neurofibrillary changes were absent on sections stained with the Gallyas silver impregnation method.

Discussion

In previous immunohistochemical studies on human brains with cerebral infarction, we reported that tau epitopes were induced differently in neurons and glial cells after an ischemic insult, where microglia/macrophages exhibited tau2 IR [24], while neurons contained Alz-50-positive granules in the cytoplasm [22]. In a subsequent study, we demonstrated that the modification of tau, linked to its immunohistochemical visualization around ischemic foci, was not necessarily related to its pathological phosphorylation [28]. In the present study, we wanted to expand this observation by examining sections from inflammatory processes of different etiologies to see whether tau2 IR is also induced in microglia/macrophages. Among the panel of anti-tau antibodies, tau2 was the only antibody that visualized the tau epitope in these inflammatory processes. The presence of the tau2 epitope exclusively in microglia/macrophages lacking neurofibrillary changes indicates that the modification of tau2 epitope in these inflammatory processes is similar to that reported for cerebral infarction [24, 28] and GCIs of MSA [21]. It is, therefore, not plausible that visualization of tau2 epitope represents an excessive

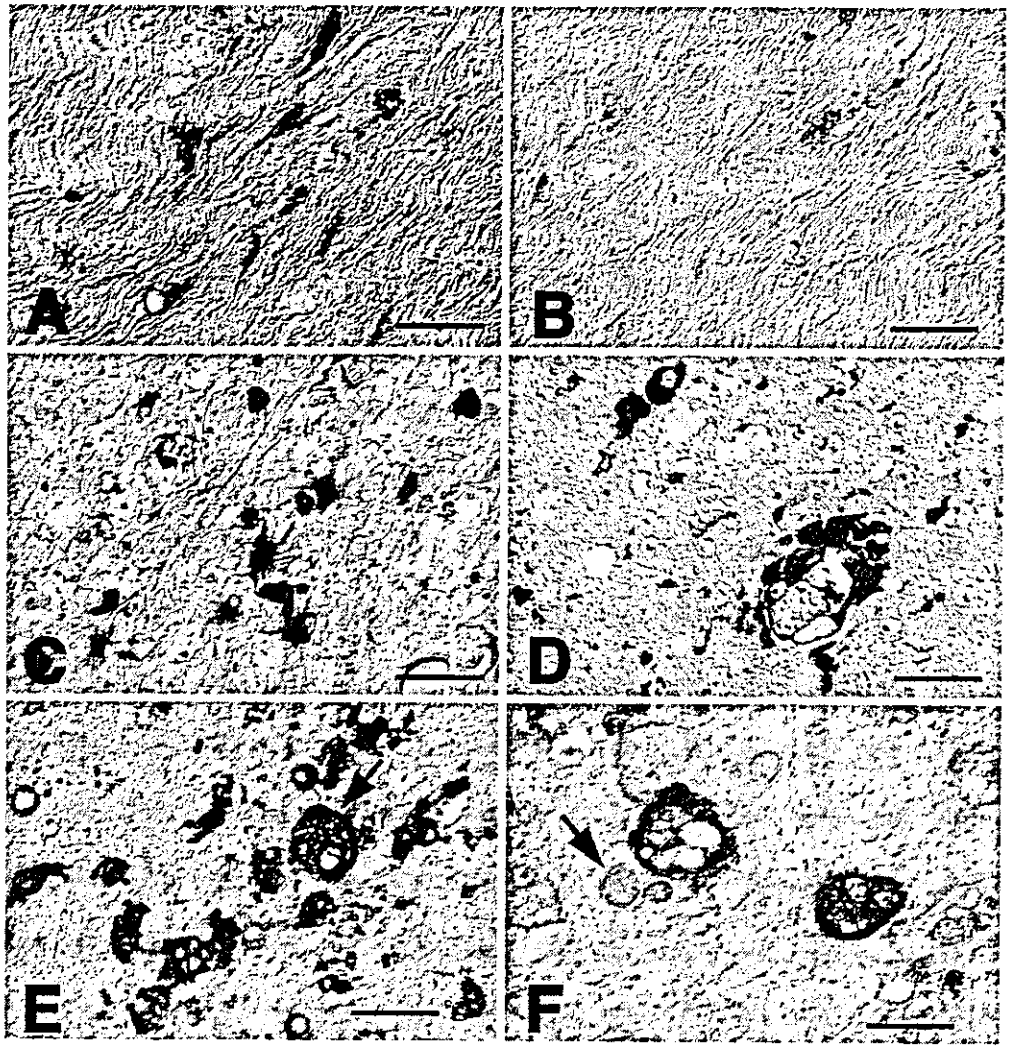

Fig. 2 A Tau2-immunoreactive glial cells at the periphery of a demyelinating focus (MS) in the internal capsule. B Co-incubation of tau2 with a synthetic peptide mimicking tau2 epitope abolishes the IR (the same area of the same case as A). C Double immunostaining with tau2 (*purple*) and an anti-GFAP antibody (*brown*) in a lesion of PML. Tau2 and GFAP epitopes are expressed in different cells without overlap. D Double immunostaining with tau2 (*purple*) and an anti-ferritin antibody (*brown*) in the white matter of the brain with HIV encephalopathy. Perivascular cells are immunopositive for both tau2 and ferritin, indicating that perivascular microglia/macrophages exhibit tau2 IR. E Double immunostaining with tau2 (*violet*) and gp24 (*brown*) in the white matter of the brain with HIV encephalopathy. Glial cells immunopositive for gp24, including multinucleated giant cells (*arrow*), exhibit tau2 IR. F Tau2 immunostain (*brown*) counterstained lightly with hematoxylin in the white matter of the brain with PML. Numerous phagosomes of macrophages are surrounded by tau2 IR, while this IR is not detectable in modified oligodendrocytes (*arrow*) (*GFAP* glial fibrillary acidic protein). *Bars* A–E 50 μm, F 25 μm

accumulation of tau. It rather indicates that modification of the tau epitope is too limited to involve the entire extent of the tau protein. Moreover, tau2 IR was restricted to the cytoplasm without extracellular deposits, which suggests its endogenous origin. Several tau epitopes, including tau2, are usually detectable on immunoblots of normal brain extract. Their immunohistochemical visualization is, however, usually difficult on sections from normal brains fixed with formalin. Tau2 antibody, however, immunolabels neurofibrillary tangles (NFTs) even after fixation with formalin [16, 17]. This discrepancy between immunoblot and immunohistochemistry is explainable if these tau epitopes in brain tissue remain active after fixation only when tau molecules are modified into a pathological state [8, 12, 18, 22, 28]. Immunohistochemical visualization of tau2 epitope is dependent on proline[101] of human tau, which was reported to be transformed into a serine-like conformation when tau protein is integrated into paired helical filaments of AD after pathological phosphorylation [11, 16, 17, 29]. One might, then, suppose that some pathological events involving tau2 epitope, not necessarily linked to phosphorylation, are responsible for its immunohistochemical visualization on formalin-fixed tissue. Indeed, this was proved to be the case in our previous studies on ischemia [28] and GCIs [21].

In contrast to neurofibrillary changes seen in AD brains, the Alz-50 IR in the cytoplasm of neurons around

the ischemic focus is granular, without fibrillary structure or argyrophilia [4, 22], as observed in pretangle neurons of the hippocampus of AD brains [3]. Tau2-immunoreactive microglia/macrophages seen in inflammatory or ischemic foci also failed to exhibit argyrophilic fibrillary features, suggesting that possible conformational changes of the tau molecule involved in these conditions are different from those of AD. Moreover, exposure to TX abolished tau2 IR in these microglia/macrophages, as observed around ischemic foci [28] and GCIs [21]. Because tau2 IR on NFTs of AD are more resistant to TX exposure [28], relative sensitivity of tau2 IR to TX shared among microglia/macrophages in ischemic foci, inflammatory processes and in GCIs is another characteristic feature of these tau2 deposits. Tau2 deposition is not a primary event in these processes. Modification of tau, with special reference to tau2 epitope, as we demonstrated in ischemia, inflammation and GCIs, is distinguishable from so-called "degenerative tauopathies". This distinction is based on a conformational change of the tau2 epitope that is reversible upon exposure to a detergent, the absence of fibrils composed of phosphorylated tau protein, and is characterized by the lack of immunohistochemical labeling by anti-tau antibodies other than tau2. We therefore propose the term "tautwopathy", to draw attention to these characteristics that are distinct from "degenerative tauopathies". If one is not aware of this distinction, immunohistochemical visualization of tau2 epitope could be confounded with degenerative tauopathy [6, 10].

We do not yet know, however, the underlying mechanisms that potentially differentiate these two distinct types of tau deposition. One possibility is that tautwopathy represents an early phase of tau deposition before fibril formation. The lack of fibrillary structure is compatible with the relative sensitivity to TX. If tautwopathy was a prelude to "degenerative tauopathy", tau deposition might precede phosphorylation. Another interpretation is that modification of tau2 epitope could be totally independent of tau phosphorylation seen in degenerative tauopathies. Preferential involvement of glial cell in tautwopathy supports this hypothesis. These two interpretations are, however, not mutually exclusive and tautwopathic processes may occur during degenerative tauopathies. Even if tau expression is a ubiquitous phenomenon irrespective of the cell type, there are still differences in tau epitopes visualized, and in the conformational states, that depend on the cell type and the disease process [23, 25, 26]. In addition, we do not know how these differences in tau deposition are brought about. Modification of or difference in the tau molecule itself (for example phosphorylation or truncation) [20], its association of other molecules [2, 7, 14, 19] or other environmental factors are possible candidates to explain these differences. Although tautwopathy is a secondary phenomenon, awareness of it will improve the understanding of the deposition of any kind tau, by providing another reference distinct from degenerative tauopathies.

Acknowledgements The authors thank Professors H. Mori (Osaka City University) and P. Davies for providing the anti-tau antibodies. This work was supported in part by the grants from the Ministry of Education, Culture, Sports, Science and Technology (grant in aid for scientific research B1530118) and from Ministry of Health, Welfare and Labor (Longevity Science H-14-005).

References

1. Adams JC (1992) Biotin amplification of biotin and horseradish peroxidase signals in histochemical stains. J Histochem Cytochem 40:1457–1463
2. Arrasate M, Peres M, Valpuesta JM, Aliva J (1997) Role of glycosaminoglycans in determining the helicity of paired helical filaments. Am J Pathol 151:1115–1122
3. Bancher C, Brunner C, Lassman H, Budka H, Jellinger K, Wiche G, Seiterberger F, Grundke-Iqbal I, Wisniewski HM (1989) Accumulation of abnormally phosphorylated tau precedes the formation of neurofibrillary tangles in Alzheimer's disease. Brain Res 477:90–99
4. Dewar D, Graham DI, Teasdale GM, McCulloch J (1993) Alz-50 and ubiquitin immunoreactivity is induced by permanent focal cerebral ischemia in the cat. Acta Neuropathol 86:623–629
5. Endoh R, Ogawara M, Iwatsubo T, Nakano I, Mori H (1993) Lack of carboxy terminal sequence of tau in ghost tangles of Alzheimer's disease. Brain Res 601:164–172
6. Forno LS, Langston JW, Herrick MK, Wilson JD, Murayama S (2002) Ubiquitin-positive neuronal and tau2-positive glial inclusions in frontotemporal dementia of motor neuron type. Acta Neuropathol 130:599–606
7. Goedert M, Jakes R, Spillantini MG, Hasegawa M, Smith MJ, Crowther RA (1996) Assembly of microtubule-associated protein tau into Alzheimer-like filaments induced by sulphated glycosaminoglycans. Nature 383:550–553
8. Grundke-Iqbal I, Iqbal K, Tung YC, Quinlan M, Wisniewski HM, Binder LI (1986) Abnormal phosphorylation of the microtubule-associated protein tau (tau) in Alzheimer cytoskeletal pathology. Proc Natl Acad Sci USA 83:4913–4917
9. Hunyaday B, Krempels K, Harta G, Mezey E (1996) Immunohistochemical signal amplification by catalyzed reporter deposition and its amplification in double immunostaining. J Histochem Cytochem 44:1353–1362
10. Kertesz A, Kawarai T, Rogaeva E, St. George-Hyslop P, Poorkaj P, Bird TD (2000) Familial frontotemporal dementia with ubiquitin-positive, tau-negative inclusions. Neurology 54:818–827
11. Lang E, Otvos L (1992) A serine → proline change in Alzheimer's disease-associated epitope tau2 results in altered secondary structure, but phosphorylation overcomes the conformational gap. Biochem Biophys Res Commun 188:162–169
12. Matsuo ES, Shin R-W, Billingsley ML, Van deVoorde A, O'Connor M, Trojanowski JQ, Lee VM-Y (1994) Biopsy-derived adult human brain tau is phosphorylated at many of the same sites as Alzheimer's disease paired helical filament tau. Neuron 13:989–1002
13. Mercken M, Vandermeern M, Lübke U, Six J, Boons J, Van de Voorde A, Martin J-J, Gheuens J (1992) Monoclonal antibodies with selective specificity for Alzheimer tou are directed against phosphatase-sensitive epitopes. Acta Neuropathol 84:265–272
14. Murayama H, Shin R-W, Higuchi J, Shibuya S, Muramoto T, Kitamoto T (1999) Interaction of alminium with PHF tau in Alzheimer's disease neurofibrillary degeneration evidenced by desferrioxamine-assisted chelating autoclave method. Am J Pathol 155:877–885
15. Nakamura A, Uchihara T (2004) Dual enhancement of triple immunofluorescence using two antibodies from the same species. J Neurosci Methods 135:67–70

16. Papasozomenos SC (1989) Tau protein immunoreactivity in dementia of the Alzheimer type. I. Morphology, evolution, distribution, and pathogenetic implications. Lab Invest 60:123–137
17. Papasozomenos SC, Binder LI (1987) Phosphorylation determines two distinct species of tau in the central nervous system. Cell Motil Cytoskel 8:210-226
18. Pollock NJ, Wood JG (1988) Differential sensitivity of the microtubule associated protein, tau, in Alzheimer's disease tissue to formalin fixation. J Histochem Cytochem 36:1117–1121
19. Sayre LM, Perry G, Harris PLR, Liu Y, Schubert KA, Smith MA (2000) In situ oxidative catalysis by neurofibrillary tangles and senile plaques in Alzheimer's disease: a central role for bound transition metal. J Neurochem 74:270–279
20. Sergeant N, Wattez A, Delacourte A (1999) Neurofibrillary degeneration in progressive supranuclear palsy and corticobasal degeneration: tau pathologies with exclusively "exon 10" isoforms. J Neurochem 72:1243–1249
21. Shibuya K, Uchihara T, Nakamura A, Ishiyama M, Yamaoka K, Yagishita S, Iwabuchi K, Kosaka K (2003) Reversible conformational change of tau-2 epitope exposed to detergent in glial cytoplasmic includions in multiple system atrophy. Acta Neuropathol 105:508–514
22. Uchihara T, Tsuchiya K, Kondo H, Hayama T, Ikeda K (1995) Widespread appearance of Alz-50 immunoreactive neurons in the human brain with cerebral infarction. Stroke 26:2145–2148
23. Uchihara T, Nakamura A, Yamazaki M, Mori O (2000) Tau-positive neurons in corticobasal degeneration and Alzheimer's disease—distinction by thiazin red and silver impregnations. Acta Neuropathol 100:385–389
24. Uchihara T, Tsuchiya K, Nakamura A, Ikeda K (2000) Appearance of tau-2 immunoreactivity in glial cells in human brain with cerebral infarction. Neurosci Lett 286:99–102
25. Uchihara T, Nakamura A, Yamazaki M, Mori O (2001) Evolution from pretangle neurons to neurofibrillary tangles monitored by thiazin red combined with Gallyas method and double immunofluorescence. Acta Neuropathol 101:535–539
26. Uchihara T, Nakamura A, Yamazaki M, Mori O, Ikeda K, Tsuchiya K (2001) Different conformation of neuronal tau deposits distinguished by double immunofluorescence with AT8 and thiazin red combined with Gallyas method. Acta Neuropathol 102:462–466
27. Uchihara T, Nakamura A, Nakayama H, Arima K, Ishizuka N, Mori H, Mizushima S (2003) Triple immunofluorolabeling with two rabbit polyclonal antibodies and a mouse monoclonal antibody allowing three-dimensional analysis of cotton wool plaques in Alzheimer disease. J Histochem Cytochem 51:1201–1206
28. Uchihara T, Nakamura A, Arai T, Ikeda K, Tsuchiya K (2004) Microglial tau undergoes phosphorylation-independent modification after ischemia. Glia 45:180–187
29. Watanabe N, Takio K, Hasegawa M, Arai T, Titani K, Ihara Y (1992) Tau 2: a probe for a Ser conformation in the amino terminus of tau. J Neurochem 58:960–966
30. Wolozin BL, Pruchnicki A, Dickson DW, Davies P (1986) A neuronal antigen in the brains of Alzheimer's patients. Science 232:648–650

Acta Neuropathologica

10.1007/s00401-004-0947-7

Regular Paper

Silver stains distinguish tau-positive structures in corticobasal degeneration/progressive supranuclear palsy and in Alzheimer's disease—Comparison between Gallyas and Campbell-Switzer methods

Toshiki Uchihara[1] ✉, **Katsuhiko Shibuya**[1, 2], **Ayako Nakamura**[1] and **Saburo Yagishita**[3]

(1) Department of Neuropathology, Tokyo Metropolitan Institute for Neuroscience, 2-6 Musashi-dai, Fuchu, 183-8526 Tokyo, Japan

(2) Department of Neurology and Psychiatry, Kanagawa Rehabilitation Center, Kanagawa, Japan

(3) Department of Pathology, Kanagawa Rehabilitation Center, Kanagawa, Japan

✉ **Toshiki Uchihara**
Email: uchihara@tmin.ac.jp
Phone: +81-42-3253881 ext 4712
Fax: +81-42-3218678

Received: 3 September 2004 **Revised:** 15 October 2004 **Accepted:** 18 October 2004 **Published online:** 24 December 2004

Abstract Possible differences in silver-staining profiles and their relation to tau-like immunoreactivity were investigated on cortical sections from corticobasal degeneration (CBD), progressive supranuclear palsy (PSP), Down's syndrome (DS) and Alzheimer's disease (AD). Pairs of mirror sections were double-fluorolabeled with an anti-PHF tau (AT8) antibody and thiazin red (TR), a fluorochrome that labels fibrillary structures such as neurofibrillary tangles (NFTs). Subsequently, one of the pair was stained with Gallyas method (GAL), and the other with Campbell-Switzer method (CS). Identification of the same structure on the corresponding microscopic fields enabled a comparison of four different profiles of each structure: AT8 immunoreactivity, and affinity to TR, GAL and CS. NFTs of DS/AD, containing three- and four-repeat tau, were positive for TR, GAL and CS. AT8-immunoreactive structures of CBD/PSP, containing mainly four-repeat tau, were positive for GAL, but negative for CS and TR. This discrepancy is explainable if the argyrophilia with GAL is related to deposits containing four-repeat tau, while that with CS is linked to those containing three-repeat tau. The lack of CS labeling may also be related to poor TR staining, possibly representing scarcity of fibrillary structure in CBD/PSP. The absence of CS staining is characteristic of tau-positive structures of CBD/PSP, which is readily distinguishable from NFTs of DS/AD, hence is of potential pathological and diagnostic relevance.

Keywords Argyrophilia - Campbell-Switzer - Diagnosis - Gallyas - Three/four-repeat tau

Introduction

Deposition of tau is a hallmark for degenerative tauopathies, currently classified according to the difference in molecular species (three-repeat or four-repeat) of pathologically phosphorylated tau [*26*]. In spite of this biochemical difference, it is still difficult to differentiate them based on the immunostaining profiles of tau-positive deposits [*5*, *6*, *10*, *21*, *37*]. Another way to identify these deposits in tauopathies is silver staining. Early observations on neurofibrillary tangles (NFTs) and senile plaques (SPs) were based on silver-staining methods. They have been used for diagnosis of these tauopathies and Alzheimer's disease (AD), and are still being improved [*1*, *2*, *7*, *9*, *13*, *16*, *17*, *23*, *35*]. Further improvements of silver-staining methods [*3*, *4*, *19*, *27*] have been claimed based on enhanced sensitivity with less background and easier standardization of the procedure. The Gallyas method (GAL) [*13*] and its modification [*4*] is one of the successful examples in clearly visualizing tau- or synuclein-containing deposits. Up to now, various silver-staining methods have been compared for their sensitivity in detecting AD-related deposits [*8*, *12*, *20*, *24*, *32*, *33*, *34*, *36*]. Among them, GAL was found to be very sensitive in detecting NFTs of AD [*20*, *24*, *33*]. The Campbell-Switzer method (CS) is also similarly sensitive [*7*, *24*]. In the present study, we applied GAL and CS to brains diagnosed as corticobasal degeneration (CBD) or progressive supranuclear palsy (PSP), and found a clear-cut discrepancy between GAL and CS. Although little is known about how these argyrophilic properties are engendered [*14*, *18*], "argyrophilia" is now found dependent not only on the sensitivity of each staining procedure but also on the disease process, and, therefore, is of potential importance in differential diagnosis of tauopathies. Moreover, this difference in argyrophilic property may possibly represent different architecture or molecular composition of the deposits.

Materials and methods

Five cases of PSP and three cases of CBD were enrolled in this study. Pathological diagnosis of PSP and that of CBD were based on the published criteria [*11*, *15*]. Additional cases of Down's syndrome (DS) and of AD were used for positive control for GAL and CS. Demographic data on these cases are shown in the Table 1. Coronal slices of cerebral hemispheres were fixed in formalin and embedded in paraffin. Large hemispheric sections were pretreated with potassium permanganate (0.3% for 10 min) followed by oxalic acid (1% for 5 min) [*27*], then stained with the GAL [*4*], and cortical areas rich in GAL-positive structures were sampled for subsequent studies. Neighboring sections from the cortical area rich in GAL-positive structures were stained either with GAL or CS [*7*], and the corresponding argyrophilic structures were compared. Mirror-section pairs (4 μm thick) from these areas were subjected to subsequent studies to identify possible relation between argyrophilia and tau-like immunoreactivity. Pairs of mirror sections were first incubated at 4° C for 2 days with an anti-PHF tau antibody (AT8, 1:10,000, Zwijndrecht, Belgium [*22*]) and the target epitope was visualized with an anti-mouse IgG conjugated with Alexa 488 (1:500, Molecular Probe, Eugene, OR). Sections were then incubated with thiazin red (TR, 1:30,000, Wako, Tokyo, Japan) for 15 min. After being observed under a confocal microscope (Leica TSC/SP, Heidelberg, Germany), one of the section pair was stained with GAL and the other

with CS to compare argyrophilic properties of each AT8- or TR-positive structure. Identification of the same microscopic field on the fluorescence images (AT8 and TR) and on the corresponding silver-stained (GAL and CS) pair-wise images allowed us to compare staining profiles of each structure based on four different properties; AT8 immunoreactivity, affinity to TR, argyrophilia with GAL and that with CS.

Table 1 Demographic data of the cases (*PSP* progressive supranuclear palsy, *CBD* corticobasal degeneration, *DS* Down's syndrome, *AD* Alzheimer's disease)

Pathological diagnosis	Cllinical diagnosis	Age at death (years)	Duration (years)	Gender
PSP	PSP	64	8	F
PSP	PSP	67	8	M
PSP	PSP	68	10	M
PSP	PSP	74	7	F
PSP	PSP	76	10	M
CBD	PSP	49	5	M
CBD	PSP	61	5	M
CBD	CBD	67	7	F
DS	DS	65		M
AD	AD	70		F

Results

On sections from DS/AD brains (Fig. 1), GAL visualized NFTs and neuropil threads (NTs) (Fig. 1A, C). On the neighboring section, CS also visualized NTFs and NTs to an equivalent extent (Fig. 1B, D). In addition, innumerable SPs were visualized with CS, while SPs stained with GAL were limited to those with neuritic reactions. On sections from PSP (Fig. 2A, C) and those from CBD, GAL-positive neurons (Fig. 2A, double arrowhead) and GAL-positive glial structures (Fig. 2A, arrows) were abundant. In contrast, CS, performed on the neighboring section (Fig. 2B,D), failed to visualize any of these GAL-positive structures. Large spherical structures, stained with both GAL (Fig. 2A, arrow) and CS (Fig. 2B, arrow), may be a neuritic plaque probably related to aging process, similar to AD. Plaque-like structure, identified on GAL-stained sections from CBD (Fig. 3A, rectangle; C) and some neurons (Fig. 3A, arrow) were not detectable on the neighboring section stained with CS (Fig. 3B, D).

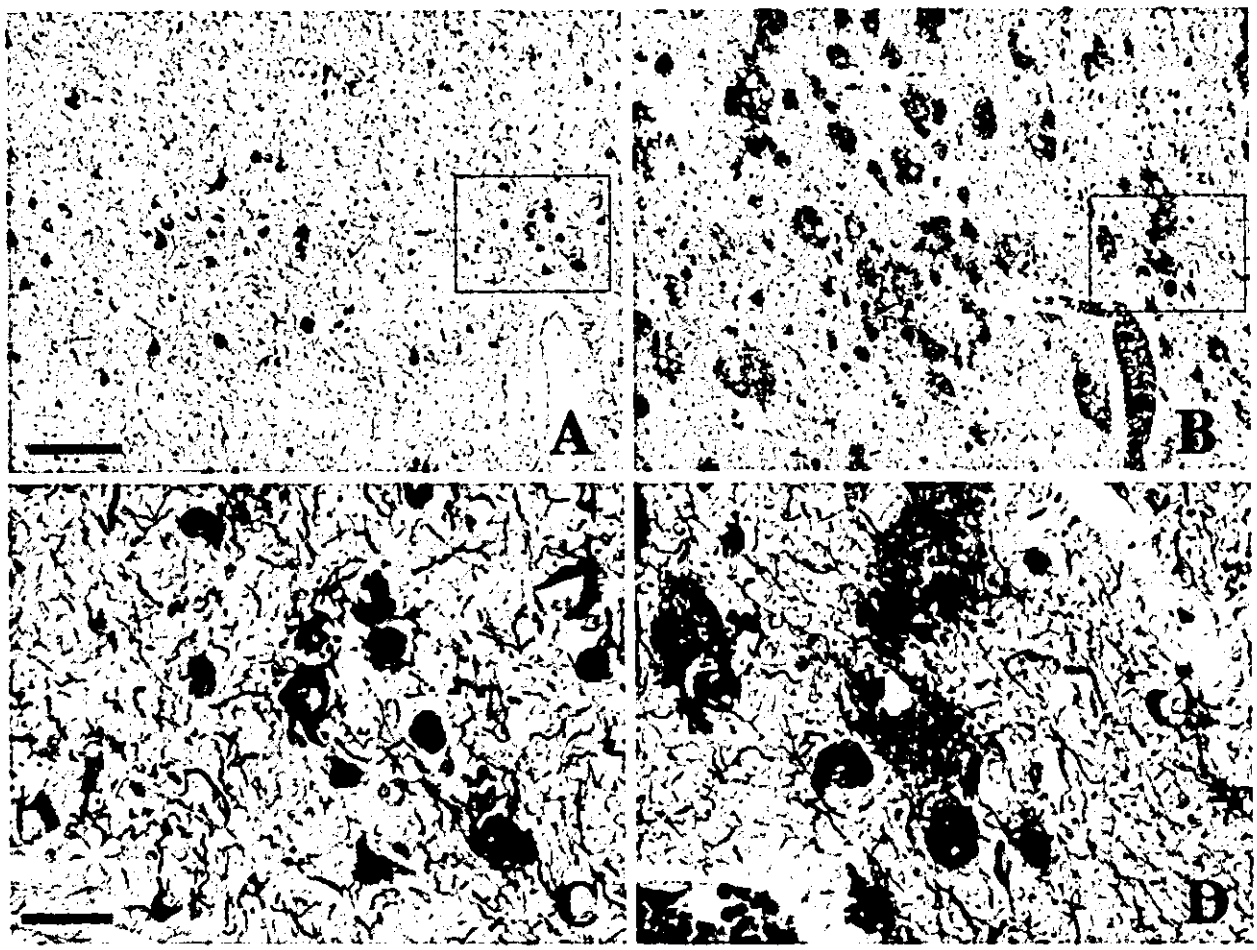

Fig. 1 Temporal cortex from an autopsied patient with DS. NFTs and neuropil threads are widespread to an equivalent extent in both GAL (**A**, **C**: higher magnification of *rectangle* in **A**) and CS-stained sections (**B**, **D**: higher magnification of *rectangle* in **B**). In addition, numerous senile plaques are detectable on CS-stained sections. *Asterisks* indicate the same blood vessels identified on the neighboring sections (*DS* Down's syndrome, *NFTs* neurofibrillary tangles, *GAL* Gallyas staining, *CS* Campbell-Switzer staining). *Bars* **A**, **B**100 μm; **C**, **D** 25 μm

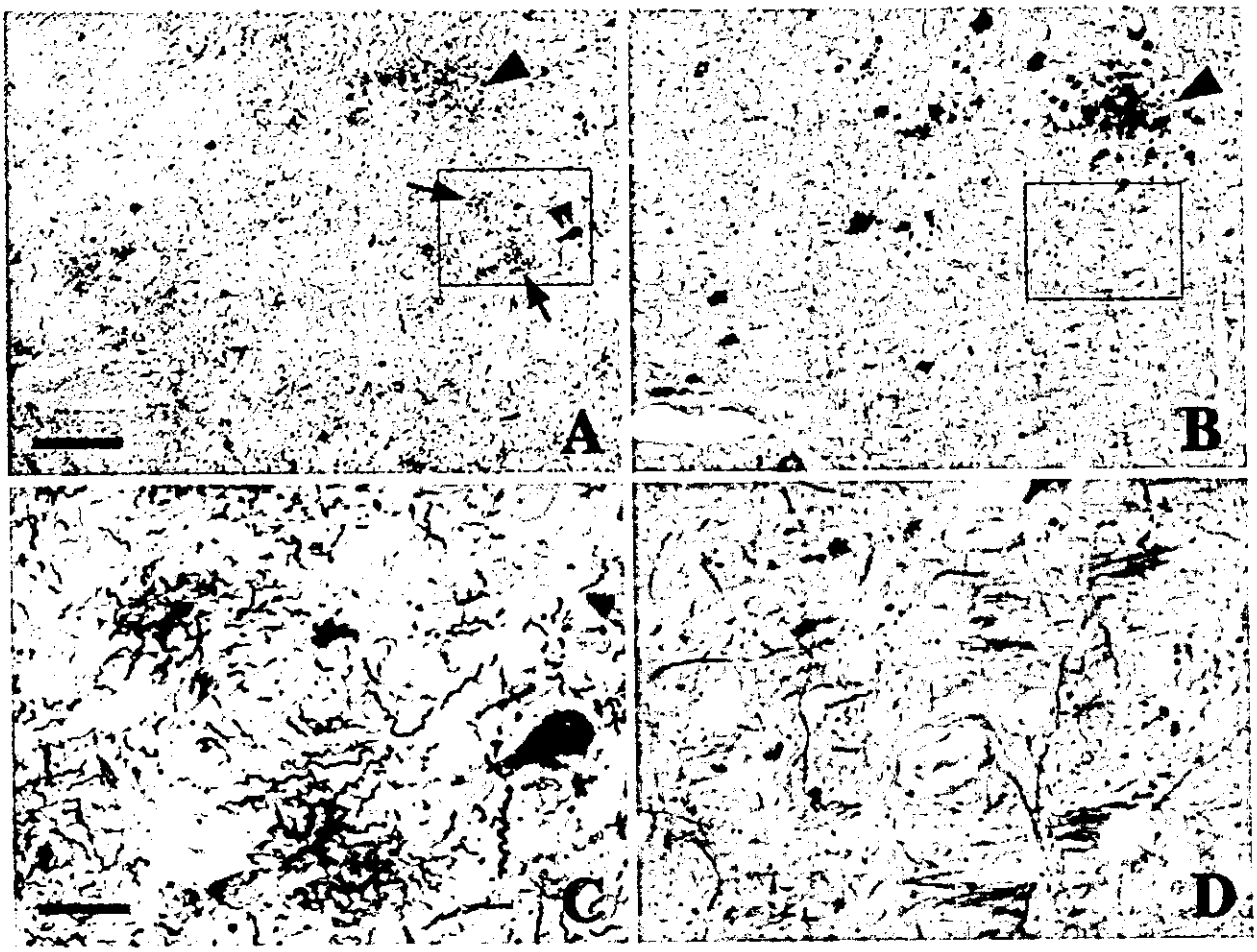

Fig. 2 Neocortex from a patient at autopsy with PSP. In GAL-stained sections (**A**, **C**: higher magnification of *rectangle* in **A**) GAL-positive neuronal (*double arrowhead* in **A**) and glial (*arrows* in **A**) components are numerous. In the same area on the neighboring section stained with CS (**B**), argyrophilic structures are limited to a larger senile plaque (**A**, **B**, *arrowhead*) probably related to aging process. Neither glial nor neuronal deposits, identified on GAL-stained sections, are detected even after CS staining is prolonged to the extent that some normal axons can be detected (**D**). *Asterisks* indicate the same blood vessels identified on neighboring sections (*PSP* progressive supranuclear palsy). *Bars* **A**, **B** 100 μm; **C**, **D** 25 μm

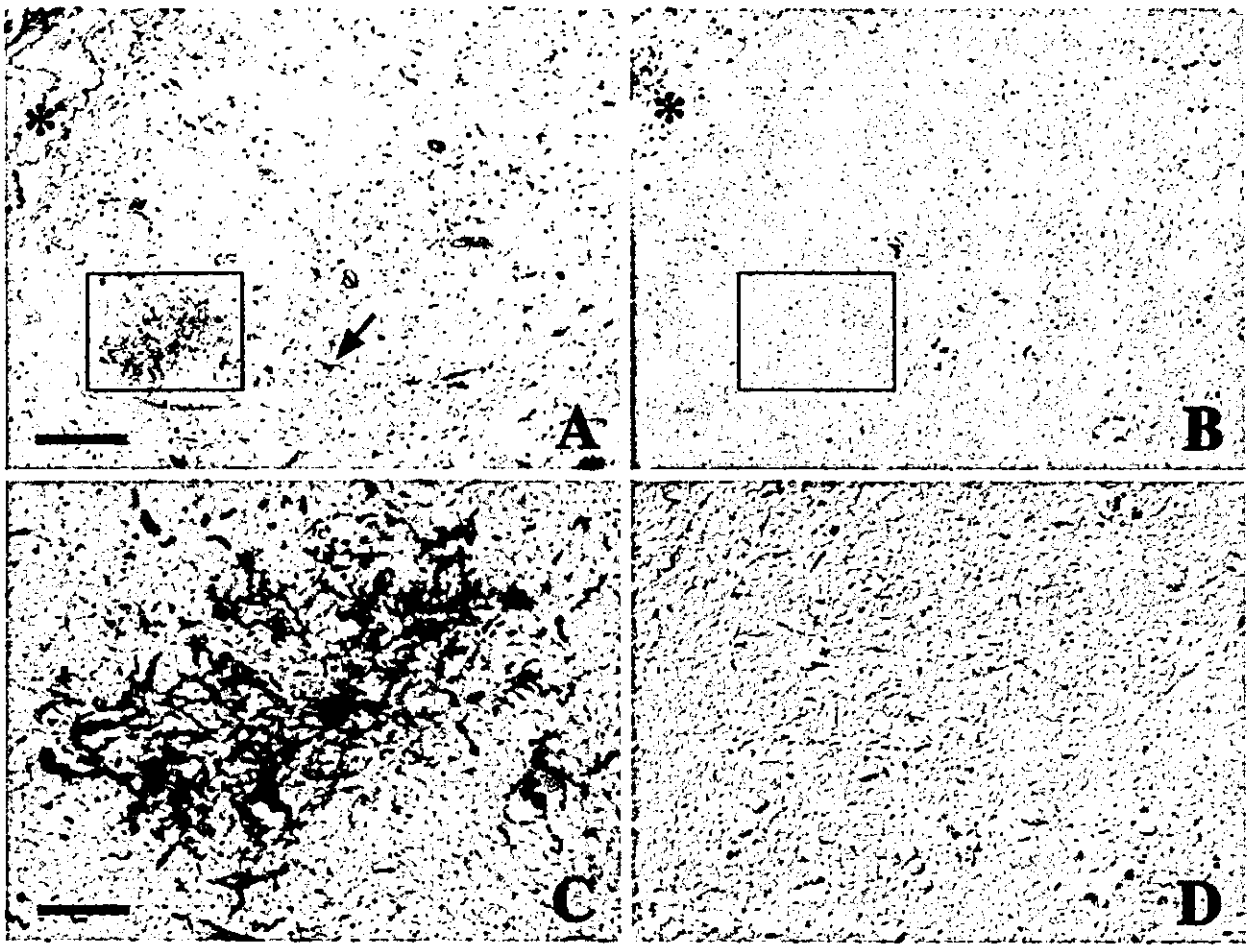

Fig. 3 Neocortex from a patient with CBD. In GAL-stained sections (**A**, **C**: higher magnification of *rectangle* in **A**), astrocytic plaques (*rectangle* in **A**, **C**) and some neurons (*arrow* in **A**) are detectable. Neither of these deposits are detected on the neighboring sections stained with CS (**B**, **D**: higher magnification of *rectangle* in **B**). *Asterisks* indicate the same pial surface on neighboring sections (*CBD* corticobasal degeneration). *Bars* **A**, **B** 100 μm; **C**, **D** 25 μm

This contrast was further confirmed on mirror-section pairs. Fluorolabeling of a mirror-section pair from AD/DS brain with AT8 and TR visualized NFTs and NTs (Fig. 4a–d), that were clearly stained with TR (red, Fig. 4c, d, asterisk) or both TR and AT8 (yellow, Fig. 4c, d, arrowhead), dependent of their evolutionary stage [*29*]. One of the section pair was subsequently stained with GAL (Fig. 4A, C), and the other with CS (Fig. 4B, D). Each of the GAL-positive structures was identifiable on the corresponding mirror section stained with CS, and vice versa. Structures positive for CS and GAL were also positive for TR or for both TR and AT8, (red or yellow, respectively, Fig. 4a–d). Another section pair from PSP brain, initially fluorolabeled (Fig. 4e–h) and subsequently silver-stained either with GAL (Fig. 4E, G) or CS (Fig. 4F, H), demonstrated that each of AT8-positive neurons (Fig. 4g, h, asterisk) was stained with GAL (Fig. 4G, asterisk). CS visualized lipofuscin granules (Fig. 4H, arrowhead) but none of the AT8-positive neurons (Fig. 4H, asterisk). Separation of fluorescence signals (AT8/green and TR/red) demonstrated that affinity to TR was evident (Fig. 4, cTR) in AT8-positive neurons (Fig. 4, cAT8) from DS brain. In contrast, it was absent or at most weak (Fig. 4, hTR) in AT8-positive neurons (Fig. 4, hAT8) from PSP. Astrocytic plaques from a CBD brain were immunoreactive to AT8 (Fig. 4i, j: green, asterisk) and similarly stained with GAL (Fig. 4I, asterisk) but not stained with CS (Fig. 4J,

asterisk).

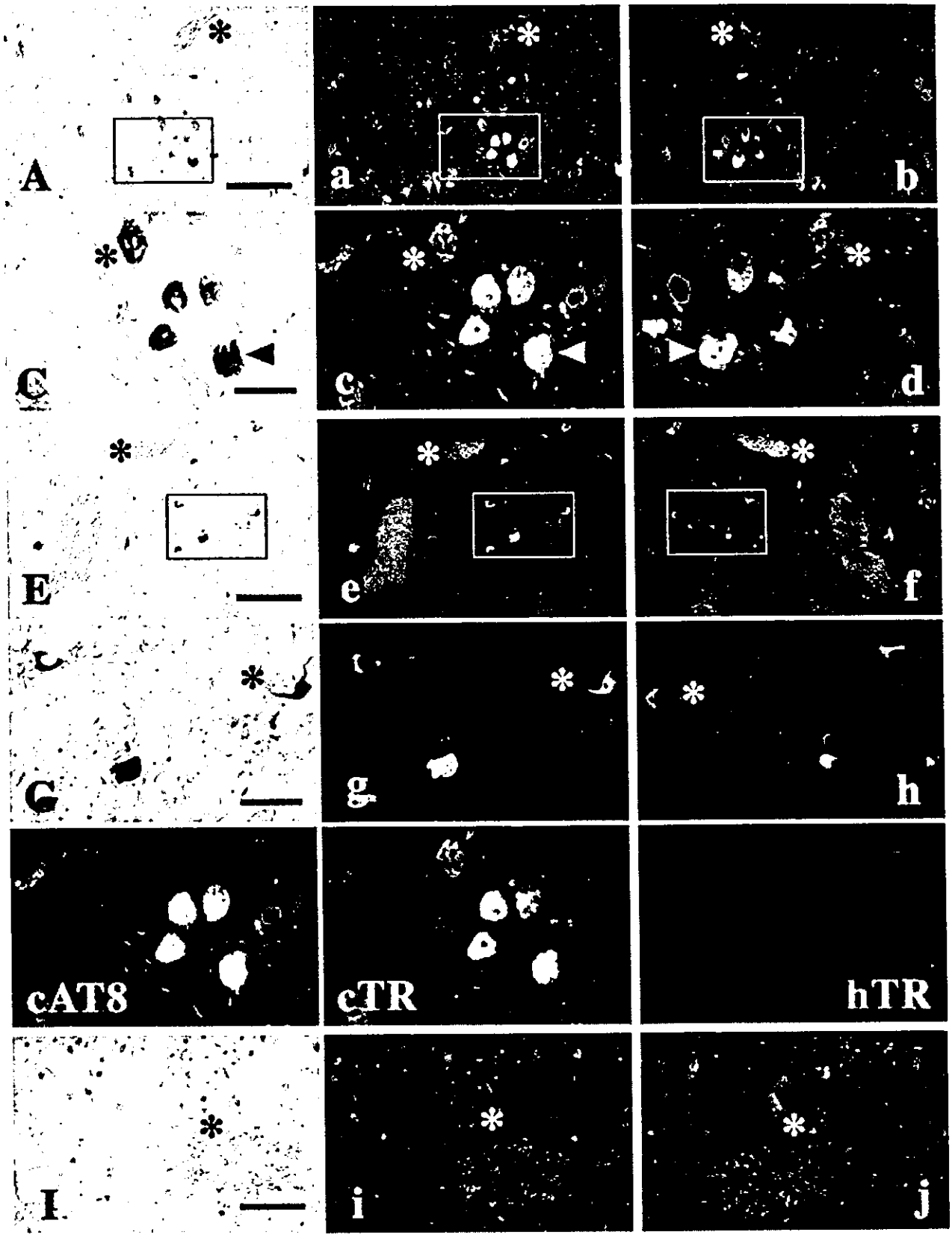

Fig. 4 Mirror-section pairs initially fluorolabeled and subsequently silver-stained. **A**, **a**, **b**, **B** A mirror section pair of the cortex from a DS patient. The same blood vessel is indicated at the top (*asterisk*). **C**, **c**, **d**, **D** Higher magnification of *rectangles* indicated in **A**, **a**, **b** and **B**, respectively. Initially double